Assessment of opto-mechanical behavior of biological samples by interferometry

Behrouz Soroushian*[a], William M. Whelan[b], Michael C. Kolios[a]
[a]Department of Physics, Ryerson University, Toronto, Canada;
[b]Department of Physics, University of PEI, Charlottetown, Canada

ABSTRACT

Optoacoustic imaging is a relatively novel biomedical imaging modality that relies on the absorption of light to create pressure transients that can be detected ultrasonically. In most scientific communications, the source of tissue contrast has been described as primarily optical. However, the thermomecahnical properties of tissue, as expressed through the Gruneisen coefficient, also affect the optoacoustic signal. To investigate the effect of thermomechanical tissue properties short pulses (~ 6.5 ns) from an optical parametric oscillator at 750 nm were used to irradiate coagulated and uncoagulated tissue-mimicking albumen phantoms, to emulate normal tissue and tissue that has been heated. The phantoms respond to the laser-induced stress by thermoelastic expansion. This thermomechanical behavior of the samples was assessed using an interferometric system capable of measuring transient displacements with a temporal resolution of less than 10 ns and a spatial resolution of < 10 nm. The experimental measurement allowed determination of the Gruneisen coefficient which is an important thermo-mechanical sample property that can affect generation of optoacoustic signals. An increase in the value of Gruneisen coefficient of 65% was measured when phantoms were coagulated compared to uncoagulated phantoms, consistent with the stiffening of the tissue mimicking material. This suggests that for thermal therapy the changes in the Gruneisen coefficient are also an important source of optoacoustic contrast.

Keywords: optoacoustic imaging, monitoring thermal therapy, laser interferometry, surface displacement measurement, Gruneisen parameter.

1. INTRODUCTION

As a minimally invasive method for treatment of tumors, thermal therapy has been examined as an alternative treatment modality by the medical research community. In this method an appropriate form of energy such as high intensity focused ultrasound (HIFU) [1], microwave radiation [2] or laser light [3] is directed to a target to locally increase its temperature. In clinical hyperthermia, treatment temperatures of 43°C - 50°C are achieved. Hyperthermia is used clinically to sensitize the cancer cells to cytotoxic agents and/or radiation. For temperatures above 50°C, tissue coagulation induces necrosis through processes such as protein denaturation which happens generally at higher temperatures, in the range of 50°C - 80°C. In either case, safety and efficacy of the treatment highly depends upon an accurate assessment of the treatment volume inside the tissue. The purpose of any such monitoring effort will be to prevent damage to the surrounding healthy tissue while providing a relatively complete coverage of the targeted region. A variety of minimally or non-invasive methods including magnetic resonance temperature imaging [4], fluoroptic temperature sensors [5] and ultrasound imaging [6] are being studied for monitoring the progression of coagulated tissue and the guidance of thermal therapy in general. However, for practical use these methods were mostly challenged either by cost of the procedure (MRI), reachable measuring depth (fluoroptic sensors and IR thermal mapping) or their lack of adequate lesion to untreated tissue contrast (ultrasound imaging).

Optoacoustic imaging, also called photoacoustic tomography (PAT) or thermoacoustic tomography (depending on the illuminating wavelengths used), is a relatively new imaging modality successfully with many biomedical applications. It relies on the detection of ultrasonic waves induced with short laser pulses in the target of interest. Optoacoustic imaging combines benefits of both optical and ultrasound imaging modalities; it provides a high spatial resolution and good contrast which are characteristics of most other optical imaging modalities while it has also a greater imaging depth because propagation of the acoustic waves in tissue is much less affected by scattering and attenuation than propagation

Photons Plus Ultrasound: Imaging and Sensing 2009, edited by Alexander A. Oraevsky, Lihong V. Wang,
Proc. of SPIE Vol. 7177, 71771X · © 2009 SPIE · CCC code: 1605-7422/09/$18 · doi: 10.1117/12.809094

of light through such optically turbid mediums. Because of such advantages optoacoustic imaging appears promising as a candidate technique for monitoring and guidance of thermal therapy.

Earlier studies have shown potential of optoacoustic techniques for detecting changes in tissue that during thermal therapy occur [7,8]. So far the changes in optoacoustic signals from thermally treated tissues are mainly attributed to changes in their optical properties, especially the drastic increase of their reduced scattering coefficient because of tissue coagulation [8,9]. The role of changes in thermo-mechanical properties of tissue is less known. Despite this, a better understanding of involved mechanisms and role of thermo-mechanical properties of tissue on optoacoustic signals is lacking.

In this study we used an interferometric measurement to detect the surface movement of samples after their irradiation by short laser pulses for assessing their thermo-mechanical behavior. The experiments were performed on normal and coagulated tissue-mimicking albumen phantoms. The results were used to quantitatively determine how coagulation causes changes in optical and thermo-mechanical properties of samples.

2. THEORY

When a short laser pulse illuminate a target, its energy will be absorbed along its path through the sample which in turn creates a small but rapid temperature increase. The resulting temperature gradient causes stresses in the bulk sample and initiates its thermoelastic expansion. The time constant of this thermoelastic expansion is proportional to the optical attenuation depth given by the ratio of 1/e depth of light absorption to the speed of sound in the sample $1/\mu_{eff}c_L$. In a turbid medium such as tissue, light is not only absorbed but also is subject to scattering. Therefore in such medium the optical attenuation depth defined by transport theory:

$$D_{eff} = \frac{1}{\mu_{eff}} = \frac{1}{\sqrt{\left[3\mu_a\left(\mu_a + \mu_s'\right)\right]}} \tag{1}$$

where μ_{eff} is the effective optical attenuation coefficient, and μ_a and μ_s' are the absorption and reduced scattering coefficients of the sample. The initial three-dimensional temperature distribution in the sample can be approximated as:

$$T_L(r,z) = T_0 \exp(-\mu_{eff} z) L(r) \tag{2}$$

in which $L(r)$ is radial profile of laser intensity and T_0 is given by:

$$T_0 = \frac{\Phi \mu_a}{\rho C_V} \tag{3}$$

where Φ is laser fluence, C_V is heat capacity at constant volume and ρ is mass density. The internal mechanical stresses created by the temperature distribution lead to thermoelastic deformations of the illuminated sample. A general equation describing the motion of the sample due to these deformations is the thermoelastic wave equation [10]:

$$\rho \frac{\partial^2 u}{\partial t^2} - \frac{E}{2(1+\nu)}\nabla^2 u - \frac{E}{2(1+\nu)(1-2\nu)}\nabla(\nabla \cdot u) = \frac{-E\beta}{3(1-2\nu)}\nabla T_L \tag{4}$$

where $\boldsymbol{u}$ is the displacement vector, E is Young's modulus, ν is Poisson's ratio, T_L is the temperature increase above a uniform ambient level because of laser energy and β is the thermal expansion coefficient. For tissue with high water content and gel phantoms the shear modulus is zero and Poisson's ratio approaches $\nu \rightarrow ½$. Also it is possible to further simplify equation (4) by considering definitions of longitudinal (c_L) and transverse (c_T) speed of sound:

$$c_L^2 = \frac{E(1-\nu)}{\rho(1+\nu)(1-2\nu)} \text{ and } c_T^2 = \frac{(1-2\nu)}{\rho(1-2)} \tag{5}$$

In liquids the transverse sound speed is zero and therefore the simplified form of equation (4) is:

$$\frac{\partial^2 u}{\partial t^2} - c_L^2 \nabla^2 u = \frac{-c_L^2(1+\nu)}{3(1-\nu)} \beta \nabla T_L \tag{6}$$

The appropriate boundary conditions must be applied to solve equation (6). The initial conditions are:

$$\begin{aligned} u &= 0 \text{ at } t = 0 \\ \frac{\partial u}{\partial t} &= 0 \text{ at } t = 0 \\ u &= 0 \text{ as } r \to \infty \end{aligned} \tag{7}$$

and for the quasi steady-state equilibrium displacement of the free surface on axis z that happen for the times greater than acoustic transient time ($t > \tau_a$ and τ_a is the time when the initial acoustic stress in the sample decays 1/e) if the initial temperature distribution is a Gaussian, a solution to equation (6) is [11] :

$$S_{eq} = \frac{2(1+\nu)}{3} \frac{\beta}{\rho C_V} g_0(R) \Phi \tag{8}$$

where $g_0(R)$ is a correction function and $R = w/D_{\text{eff}}$ where w is the beam radius. This function includes a first-order Bessel function and is an indication for ratio of laser beam radius to the effective attenuation depth in the target.

3. METHODS AND MATERIALS

3.1 Interferometer system

The surface displacements were measured using a modified Michelson interferometer originally proposed by Dark and her coworkers [10]. The interferometric probe beam is provided by a cw solid-state laser (CrystaLaser GCL-025-S) at a wavelength of 532 nm. The laser is capable of delivering a maximum output power of 25 mW. Light from the laser is divided in two parts by a beam splitter. In the sample arm of the interferometer one part of it is focused onto the target by a 5 cm lens. The light reflected from the target is recollimated by the lens and returns to the beam splitter. The other part of the laser light passes through a 25 cm lens and a corner cube, before being focused on a reflecting mirror. This mirror is adjusted in a way that light travels back to the corner cube, is recollimated by the lens and goes back to the beam splitter. On the beam splitter the light from both arms, reference and target, is combined and directed toward a photomultiplier tube (Hamamatsu H7732P-11) for detection. An absorptive color filter allowing passage of a narrow band around 532 nm is placed in front of the photomultiplier to filter out any stray light. Electric signal from the photomultiplier tube (PMT) is amplified by an amplifier (Miteq AU-1291, 0.01-500 MHz) and digitized by an oscilloscope (Agilent DSO6054A – 500 MHz). Since the corner cube rotates with a constant frequency of 5 Hz, the reference arm path length changes at a constant rate. This creates an interference fringe pattern whose frequency is constant when the sample is not moving. Any movement of the sample's surface modulates the frequency of the fringe pattern. By using the Hilbert transform it is possible to find the complex signal of the resulting interferogram and from there to determine the target displacement [12].

To create the thermal expansion in the target, light pulses from a Vibrant B 532 (Opotek Inc., Carlsbad, CA, USA) laser are used. The system is fed by a Q-switched Nd:YAG laser at 1064 nm with a pulse duration of ~6.5 ns and a repetition rate of 10 Hz. The maximum output power of the Nd:YAG laser is 800 mJ/pulse with a beam diameter of ~9 mm. The pulses from this laser directed into an optical parametric oscillator (OPO) which provides output wavelengths tunable in a range between 680 and 950 nm. The OPO is capable of delivering a maximum power output of 75mJ/pulse at ~710nm.

The light beam from the OPO is collimated by a lens and through mirrors is directed toward the target. Before reaching the target a portion of the beam is separated by a glass plate and reflected on a biased high speed silicon photodiode (Thorlabs, DET10A, 200-1100 nm, 1 ns rise time) for measuring energy of each pulse and providing a trigger signal for data acquisition. The remaining light passes through a shutter and by a 5 cm lens is focused on the target. The final size of the beam at the target position is measured by its burned trace on a photographic paper. It is found that the beam has an elliptical cross section with respectively major and minor axis of 5 and 3 mm on the sample.

3.2 Tissue equivalent albumen phantoms

Albumen-based phantoms are widely used as tissue mimicking mediums in studies of laser irradiation. The phantoms are homoheneous and have a uniform appearance. The albumen phantom like tissue coagulates when heated. Albumen is comprised mainly of water (88.1%), globular proteins (10.2%) and lipids (0.05%) and is commercially available in powdered form. To achieve optical properties that are more closely matched to tissue, Naphthol Green dye is used to increase the phantom's optical absorption in short near infrared (700 – 850 nm) and a polysaccharide agar gel is used to increase its optical scattering and its stiffness. Agar also acts as a solidifying agent making it more conducive to thermal measurements of bulk specimens. Four phantoms were made using this mixture and following the procedure previously described by Iizuka *et al* [9]. The experiments were conducted in two different days. Each day two phantoms were prepared. One of them was heated and the other one was used without heating. The phantoms were prepared in aluminum cylindrical containers with a diameter of 2.5 cm. Then one of the pair was sealed and immersed in a hot water bath at 70°C for 20 minutes. As expected, visible whitening was observed in the heated samples indicating denaturation of their albumen proteins. The heated phantoms were then cooled down to the room temperature and with non-heated ones were used in the interferometric measurements.

4. RESULTS

Samples were placed in front of interferometric system. The fringe pattern from the stationary samples was maximized by fine tuning of the optical alignment. By using electronic signals from the photodiode data acquisition was synchronized with incident pulses from the OPO. The OPO was adjusted to operate at a wavelength of 750 nm. When a single pulse is absorbed by the phantom (beginning at 0 ns), the absorbed energy generates thermoelastic stresses within the sample. These stresses propagate through the phantom and cause a surface displacement which is measured by interferometry. Measurements were performed for 6 levels of pulse energies from the OPO. However because of relatively high fluctuation of pulse energy from the OPO for each individual pulse, the energy of each pulse was separately measured and data acquired from the shots with similar pulse energies were arranged in separate bins. Hence the number of signals collected and analyzed in a bin varied. Surface displacements calculated from the signals in the same bin were averaged and the result was considered representative of the average pulse energy that was measured for the data collected in that bin. Sample displacement traces after binning for each of the four phantoms are shown in Fig. 1.

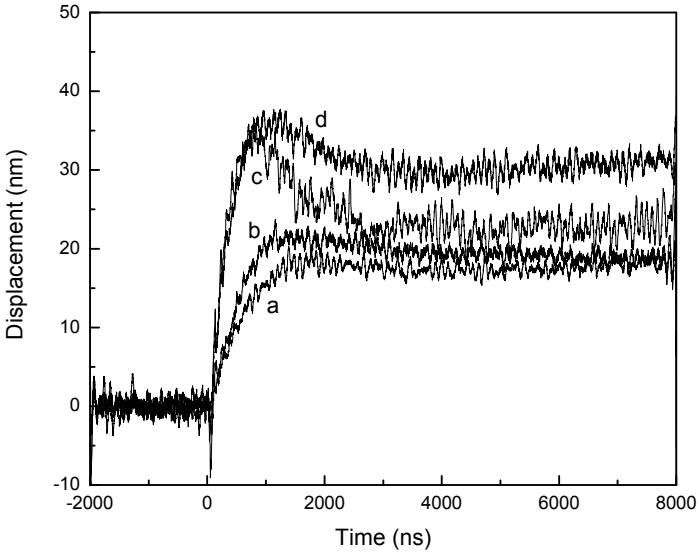

Fig. 1. Traces of surface displacement for four albumen phantoms (a,b uncoagulated – c,d coagulated) after their illumination by an 8 ns laser pulse at 750 nm. The traces are result of averaging over 10 (a) and 7 (b, c, d) signals in an energy bin.

The sample surface expands in response to the stress induced by energy absorption. For the uncoagulated samples the surface expansion reaches its maximum between 1180 and 1400 ns after incident laser pulse, while the coagulated samples expand faster and reach their maximum expansions between 800 and 930 ns after the laser pulse. The optical attenuation depth D_{eff} decreases with coagulation. This trend is in agreement with previous work demonstrating an increase of effective attenuation coefficient because of phantom coagulation [9].

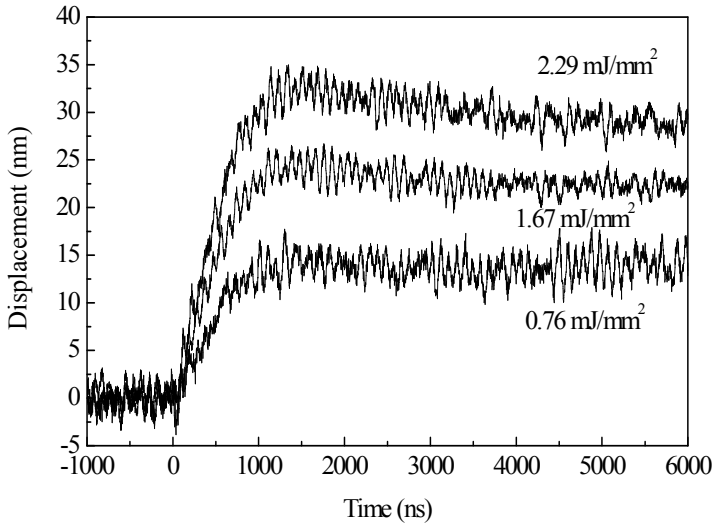

Fig. 2. Traces of surface displacements for an uncoagulated albumen phantom after irradiation by 8 ns laser pulse at 750 nm versus different averaged laser fluences.

Sample surface displacements of one uncoagulated phantom for different average pulse fluences are shown in Fig. 2. Higher laser fluences cause bigger displacements. The coagulated phantoms showed bigger maximum expansion of 51 nm when compared with 32 nm maximum expansion for the uncoagulated phantoms for similar fluences. The magnitude of thermoelastic expansion of the phantoms is linear with laser fluence and is given by equation (8) [13]:

$$S_{eq} = \frac{2(1+\nu)}{3}\frac{\Gamma}{\rho c_L^2} g_0(R)\Phi \,. \tag{9}$$

where the Gruneisen parameter is defined in terms of thermal expansion β and sample's constant volume heat capacity C_V as:

$$\Gamma = c_L^2 \beta \Big/ C_V \tag{10}$$

We assume that in our experiments the Poisson's ratio is ½ and the speed of sound is close to that of water: 1500 m/s. Moreover, we assume the density of sample is 1000 Kg/m^3 and a correction factor $g_0 = 0.6$ (since the beam radius is 3 mm). Although in equation (9) S_{eq} is the equilibrium displacement when the stresses in the sample are passed, in our analysis we considered the maximum displacement of the phantoms surface for calculating the Gruneisen coefficient.

Fig. 3. shows the maximum displacement versus laser fluence for four phantom samples. Linear regressions forced to pass through zero displacement for laser fluence of zero was calculated for each data set. The Gruneisen coefficient for each sample was estimated using the slope of these lines in the equation (9).

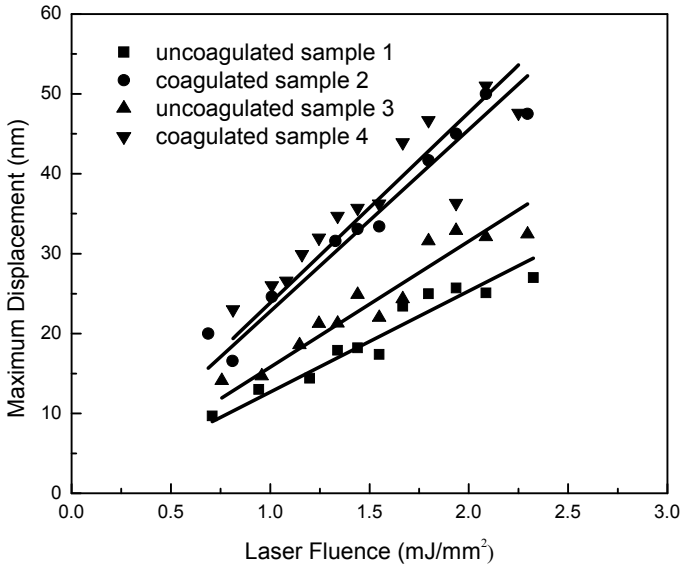

Fig. 3. Maximum displacement of albumen phantoms versus average laser fluence. The solid lines are linear regression forced to pass through the (0,0) point for each data set.

We found values ranging from 0.048 and 0.06 for the Gruneisen coefficient of uncoagulated samples while the values for coagulated phantoms ranged from 0.087 and 0.091. These results indicate an increase of approximately 65% in value of the Gruneisen coefficient when the phantoms are coagulated.

5. CONCLUSION

Interferometric measurements of surface displacement for albumen tissue-mimicking phantoms after irradiation by short laser pulses were performed. The results were used to estimate values of the Gruneisen coefficient for the samples. Moreover characteristics of the sample response to laser irradiation were assessed. It was found that in addition to the changes occurring in the phantom's optical properties because of its coagulation, its thermo-mechanical properties, which are mainly characterized by Gruneisen parameter, also undergo significant changes. We observed and increase of Gruneisen coefficient following coagulation of the phantoms. Further experiments on tissue equivalent phantoms and eventually *ex-vivo* biological samples are planned to better characterize the extent of these changes and their relevance to thermal therapies.

ACKNOWLEDGMENT

The authors would like to gratefully acknowledge Arthur Worthington for his assistance in the experiments and Dr. J. Carl Kumaradas and Dr. Sankar Narasimhan for valuable input. Financial support was provided by the Natural Sciences and Engineering Research Council of Canada and the Canadian Institutes of Health Research (grant CHRPJ323745-60) and the Canada Foundation for Innovation (CFI). This research was undertaken, in part, thanks to funding from the Canada Research Chairs Program awarded to Michael Kolios.

REFERENCES

[1] Kennedy J. E., Ter Haar G. R. and Granston D., "High intensity focused ultrasound: surgery of the future?" Br. J. Radiol. 76, 590-599 (2003).

[2] Vargas H. I., Dooley W. C., Gardner R. A., Gonzalez K. D., Venegas R., Heywang-Kobrunner S. H. and Fenn A. J., "Focused microwave phased array thermotherapy for ablation of early-stage breast cancer: results of thermal dose escalation", Ann. Surg. Oncol. 11(2), 139-146 (2004).
[3] Whelan W. M., Davidson S. R. H., Chin L. C. L., Vitkin I. A., "A novel strategy for monitoring laser thermal therapy based on changes in optothermal properties of heated tissues", International Journal of Thermophysics 26(1), 233-241 (2005).
[4] Rieke V., Pauly K. B., "MR Thermometry", J. Magn. Reson. Imaging, 27, 376-390 (2008).
[5] Reid A. D., Gertner M. R., Sherar M. D., "Temperature measurement artefacts of thermocouples and fluoroptic probes during laser irradiation at 810 nm", Phys. Med. Biol. 46, N146-N157, (2001).
[6] Anand, A., Savéry, D., Hall, C. S., "Ultrasonic determination of three-dimensional spatial and temporal thermal distribution for therapy monitoring", Proc. IEEE International Conference on Acoustic, Speech and Signal Processing, 2, II1108-II1111 (2006).
[7] Larin K. V., Larina I. V. and Esenaliev R. O., "Monitoring of tissue coagulation during thermotherapy using optoacoustic technique", J. Phys. D: Appl. Phys. 38, 2645–2653 (2005).
[8] Castelino R. F., Whelan W. M. and Kolios M. C., "Photoacoustic detection of protein coagulation in albumen-based phantoms", Proc. SPIE 6856, art. number 685626 (2008).
[9] Iizuka, M.N., Sherar, M.D. and Vitkin, I.A. "Optical phantom materials for near infrared laser photocoagulation studies", Lasers in Surgery and Medicine 25, 159-169 (1999).
[10] Landau L. D. and Lifshitz E. M., "Theory of elasticity", Oxford Pergamon, 3rd Edition (1986).
[11] Albagli D., Dark M., von Rosenberg C., Perelman L. and Itzkan I., "Laser-induced thermoelastic deformation: A three-dimensional solution and its application to the ablation of biological tissue", Medical Physics, 21(8), 1323-1331 (1994).
[12] Harkin J. P. and Flavin D. A., "Interferometric displacement tracking based on Hilbert transform processing", Proc. SPIE 4204, 89-98 (2001).
[13] Dark M. L., Perelman L. T., Itzkan I., Schaffer J. L. and Feld M. S., "Physical properties of hydrated tissue determined by surface interferometry of laser-induced thermoelastic deformation", Phys. Med. Biol., 45, 529-539 (2000).